A major purpose of the Technical Information Center is to provide the broadest dissemination possible of information contained in DOE's Research and Development Reports to business, industry, the academic community, and federal, state and local governments.

Although a small portion of this report is not reproducible, it is being made available to expedite the availability of information on the research discussed herein.

1

LA-UR-83-3701

LA-UR--83-3701

DE84 004414

CONF-831195--4

TITLE: THE INFLUENCE OF A PLASMA DURING LASER WELDING

AUTHOR(S): R. D. Dixon, MST-6
G. K. Lewis, MST-6

SUBMITTED TO: The Proceedings of the Int-Congress on Lasers and Electro Optics, Los Angeles, CA, November 1983.

Los Alamos

Los Alamos National Laboratory
Los Alamos, New Mexico 87545

The Influence of a Plasma during Laser Welding

R. D. Dixon and G. K. Lewis

Los Alamos National Laboratory

P.O. Box 1663, MS G770

Los Alamos, NM 87545

Abstract

High speed movies of single pulse laser welds are correlated with optical emission from the plasma and the acoustic wave to study and model enhanced coupling. The movies and acoustic signals combine to support enhanced coupling through the development of a laser supported combustion wave.

Introduction

During recent years laser welding has become an acceptable and reliable processing tool for the fabrication industry. It has found application in areas where conventional processes are not able to perform the work because of heat input, distortion, vacuum, location, etc. Commercial laser welding systems are available with a few Watts of Pulsed 1.06 micron (μ) wavelength radiation from a Nd-YAG Laser to Multi-Kilowatts of continuous (cw) 10.6 μ wavelength radiation from a CO_2 laser. These systems are capable of melting nearly all types of metals and alloys.

Although the process is gaining widespread acceptability it still produces welds having a high variability in morphology. This is particularly true of metals and alloys with high intrinsic reflectivity such as gold, aluminum and copper as well as those like stainless steel which have (in most cases) lower reflectivity. These facts, along with the appreciation that the laser produced plasma resulting from the laser-material interaction could significantly influence the heat input, and perhaps explain acoustic emission results lead to the current work. Further it was recognized that the plasma could not be readily controlled to produce a better weld or less weld variability.

This report describes work performed to characterize the plasma and its influence upon laser material interactions. The model presented is an extension of the model created to explain laser damage.[1,2] This model shows that under proper conditions the plasma is responsible for the major heat input to a part. This phenomenon is known as "enhanced coupling" and the conditions leading to it are discussed below. This report extends the model for plasma generation leading to enhanced coupling to the long pulse lengths used in welding and presents data to support it. This report is a continuation of work presented earlier and serves to amplify and support the model.[3,4]

Plasma Generation and effects

The laser-material interaction is initiated by the absorption of laser radiation at the material surface which results in an increase in temperature. This is not an efficient process for 1.06 μ or 10.6 μ radiation because many materials are reflective at these wavelengths as shown in Fig. 1. Additionally photoelectric and thermoelectric processes occur which yield an increase in electron density near the surface. It is also likely that the incident radiation is of sufficient energy density that it will vaporize surface asperities which will contribute material atoms, thermal electrons and ions to the near surface region. All of these processes serve to increase the electron, ion and neutral atom density (plasma) near the surface to the point where the laser radiation is absorbed by these particles. The heat input to the material is now complemented by the plasma.

In general the definition of a plasma is a gas of free positive and negative charges, a condition probably reached before the absorption of the laser radiation. However, this point is not critical because the lifetime of free charges in an atmosphere of gas is very short. Thus the free charges must be generated at a rate sufficient to produce a free charge density which will absorb the laser radiation. When this occurs the plasma is said to be initiated which simply refers to its observability on a microscopic scale.

Another feature critical to determining if the plasma formed will contribute significantly to the heat into the material is the pressure wave created when the plasma begins to absorb laser radiation.[1] Because of the temperature rise in the plasma upon absorption of the laser radiation and the presence of the material surface a pressure wave is generated and propagates along the laser beam axis. As the plasma continues to absorb energy and increase in temperature it begins to move into the surrounding region via radiation. In general the motion is one-dimensional along the beam axis since the energy is being supplied there. These conditions describe a Laser Supported Absorption (LSA) wave.[1]

The absorption wave can be either a Laser Supported Combustion (LSC) wave or a Laser Supported Detonation (LSD) wave depending upon the hydrodynamics.[1] In all cases the LSA wave propagates into a region of gas that has been shocked by the precursor pressure wave. If the LSA wave velocity is subsonic and less than or equal to the gas particle velocity the LSA wave is said to be a LSC wave. If the LSA wave is supersonic it will then travel with the shock wave and is known as a LSD wave. This nomenclature is based on the similarity in hydrodynamics and not the actual combustion or detonation processes. Figure 2 illustrates phenomonologically these two waves and the corresponding conditions.

The above model also illustrates the need for a threshold energy since sufficient energy must be input to create a plasma which can absorb the incident laser radiation. Also, the type of wave generated depends upon the incident power density. Incident high fluence short duration radiation would produce a large free charge generation rate, rapid radiation absorption by the plasma, high plasma temperature, rapid plasma expansion, supersonic shocks and thus a LSD wave. Incident radiation with lesser fluence and/or longer duration yet still greater than threshold would produce a LSC wave with all other factors such as material and environment constant. The transition between a LSC and a LSD wave will occur somewhere between the extremes and can be influenced by the material as well.

From a plasma radiation standpoint a LSC wave is expected to contribute more radiant energy to a material than an LSD wave.[2] A LSC wave will have less mass flow, remain one-dimensional longer, remain close to the target surface, have larger dimensions, and be less transparent than a LSD wave, by virtue of its slow velocity. Thus to maximize the energy to a target it is beneficial to create a LSC wave.

The energy absorbed by the target is essentially controlled by the absorption. From figure 1 it is seen that the absorption increases (decrease in reflectivity) as the wavelength decreases. A high temperature plasma will radiate wi[illegible] body spectrum and therefore the higher the temperature the greater the total radiation, but more importantly the greater the amount of short wavelength radiation. Model calculations show that LSC waves typically reach temperatures of 5,000 to 20,000°k and thus are rich in high energy radiation.[2,3]

Processes such as conduction, convection and Bremsstralung can also contribute to target heating. These processes are calculated to contribute less than 5% of the incident power each, while radiation has been calculated to contribute up to 50% of the incident power.[2] Heat input as a result of radiation from a plasma then constitutes a significant factor in laser processes (in some cases an increase greater than an order of magnitude over absorption at the laser wavelength).

Results from calculations of one dimensional LSC wave propagation show that after ignition by a 1×10^5 watt cm^{-2} CO_2 laser pulse a LSC wave will travel 2 cm in less than 100 μ sec.[5] Two-dimensional LSC wave calculations for 1×10^6 watt cm^{-2} CO_2 laser radiation show that a high temperature isotherm closes on itself within 2-3 cm of the surface in less than 100 μsec also.[5] Most laser welding operations utilize pulse lengths in excess of 100 μ sec. Based on this one expects several LSC waves to be generated, propagate and decay during one welding pulse. From a heat input standpoint the physical parameters of each wave are of fundamental interest. However, it is appreciated that in order to do these calculations the initial gas state must be known for each wave. Since each wave will depend upon the previous one it is impossible to do this calculation. It is sufficient though to anticipate that the creation of each LSC wave is signaled by a precursor shock wave and the subsequent plasma ignition. Measurement of these velocities will determine whether the plasma waves are LSC or LSD and thus allow estimates of the effective heat input.

In summary, enhanced coupling occurs when a LSC wave is generated and numerous LSC waves are expected during one welding pulse. The enhanced coupling can be as large as 50% of the incident laser power. The ramifications of this are that by proper tailoring of the Laser pulse to produce and maintain a LSC wave near the target surface very large amounts of energy could be coupled into the part. In order to achieve this it is essential to know what type of plasma is generated and how it behaves. The next section describes the experimental work done to determine the plasma type.

Experimental

Two 3.175 mm diameter condensor microphones were used to measure the velocity of the precursor pressure wave. This measurement defines whether the plasma is combustion (subsonic velocities) or detonation (supersonic velocities). The microphones were placed at different distances from the impingement point and the velocity calculated from the ratio of the difference in separation to the difference in arrival time. The microphones were placed such that they would not interfere with the plasma or each other. Because we are unable to calibrate the microphones only velocity was measured and not pressure.

A photomultiplier tube (PMT) with an S-20 response was used to detect the onset of radiation from the plasma. The PMT was coupled to the plasma radiation using a 0.25 mm diameter optical fiber.

The laser temporal pulse shape was monitored using a silicon photodiode at the rear of the laser cavity. This provided the reference to which all observations were made as well as the trigger to initiate data acquisition. Within the field of view of the fiber this data can be used to signal plasma formation.

Several data were taken of the current from the target using a high gain current amplifier.

A high speed video recorder, with two synchronized cameras, was used to observe the initiation, propagation and decay of the plasmas generated and to substantiate the initiation times obtained using the PMT signal. The picture from one camera could be inset in the video display of the other. A triggered flash lamp was focused into one camera and thus provided the reference mark for the video. This data provides evidence of multiple LSC wave generation and a rough estimate of the wave velocity. The velocity was determined by measuring the distance a front had moved during one frame. The data were taken at 2,000 frames per sec with each frame divided into six pictures to produce 12,000 pictures per sec. No shutter was used, thus, each picture had an exposure of 83 1/3 microsec.

All devices were triggered by a pulse generated when both the laser shutter was open and a laser pulse occurred. All electronic data were recorded at 1 or 2 μ sec per data point using either a 2 and/or a 4 channel digital storage scope with floppy disc storage media. The trigger pulse triggered one or both scopes depending on the number of parameters being monitored, a delay pulse generator if needed and a flash lamp. The delay pulse generator was used only if records were taken using both scopes and was routed into one channel of each scope to provide an accurate reference for event comparisons.

The laser used was a pulsed Nd-YAG (1.06 μ wavelength) laser with a maximum power of 400 watts. The pulse length could be varied from 0.5 to 8.5 m sec. All data were taken at sharp visual focus. The power was measured several times for each condition using a calorimeter. Only one laser pulse was used for each data point.

All targets were 22.2 mm in diameter by 1.5 mm thick discs mounted on a rotary base. The rotary base allowed precise indexing of the target and provided a common radius for cross sectioning by diamond knife machining. The diameter of the weld was measured at the surface and the weld then sectioned at its center to measure the depth of penetration. The materials used were 6061 Al, 5052 Al, 1100 Al and 304 stainless steel. Table I shows the matrix of experimental conditions.

Table I

Experimental Conditions[1]

Material	Average Power	Pulse Length
304 Stainless Steel	370 watt	7.8 ms to 3.6 ms
1100 Al	to	
6061 Al	20 watt	
1100 Al		

1. The power and pulse length used on each material depended upon the creation of a visible melting.

Results and Discussion

Data were taken using laser pulse lenghts of 7.8 msec, 5 msec or 3 msec. The pulse lengths were determined by the zero voltage crossings and not full-width-half-maximum type measurements. A typical laser pulse is shown in figure 3. The laser was adjusted to produce 10 pulses sec^{-1} and to initiate only one pulse when the shutter was open. Average power measurements were made by firing into a calorimeter.

The velocity of the precursor pressure wave was measured on all materials at high, intermediate and low power levels. At the highest powers (360w to 370w), the velocity was approximately the sound velocity for plasmas on 304 stainless steel (SS) and 6061 Al. The velocities measured for 1100 Al and 5052 Al at 370 watts were 27,000 cm sec^{-1} and 17,000 cm sec^{-1} respectively. Pressure wave velocities could be measured from the stainless steel plasma down to powers of 100 watt but there was insufficient signal to measure the velocities from Al below about 250 watt. At 100 watt the velocity from the stainless steel plasma pressure wave was approximately 8,000 cm sec^{-1}. The velocities for 1100, 5052 and 6061 Al at 300 watts were 5,000, 12,000 and 25,000 cm sec^{-1} respectively. There was no measurable velocity from 1100 Al below 250 watts and although there were signals from the 6061 and 5052 Al below 200 watts it was not possible to accuratly determine velocities. In all cases where multiple data were taken, the standard errors ranged from 4,000 cm sec^{-1} to 12,000 cm sec^{-1}. It is noteworthy that the standard error was greatest from data taken on stainless steel which was the only material yielding pressure wave velocities down to powers less then 100 watts. Figure 4 is an example of the type of data obtained from these measurements. For the limited amount of data taken at pulse lengths less than 7.8 msec it appears that the pressure velocity is independent of pulse length. Because all velocities measured were less than or equal to the velocity of sound the plasmas generated are combustion types. This confirms that the absorption wave is a LSC wave.

An example of the PMT data is shown in figure 5. This data is used to determine the plasma initiation time for each material, and, to a limited extent the number of plasmas generated during one laser pulse. The plasma initiation time is determined by the first inflection point in the PMT signal while the number of plasmas is determined by the number of maxima. Since the plasma is expanding and moving away from the surface and the PMT fiber has a limited field of view, the structure of the PMT signals shows both initiation and motion effects. It does however graphically demonstrate that multiple plasmas are occurring.

Figure 6 shows the plasma initiation times for 304SS, 1100 Al and 6061 Al versus power for 7.8 msec pulse lengths. For these data the initiation time was taken as the first inflection point in the PMT signal. Figure 6 shows that low powers require longer initiation times with the time decreasing as the power increases. It also shows that more power is required to initiate a plasma on the Al alloys than on stainless steel. Examination of the plasma initiation times for the Al alloys does not reveal any obvious dependence on the alloy type. It is expected that the initiation times will be different but the magnitude is not known. In order to determine the alloying effect additional data must be taken.

Figure 7 shows the current emitted from a 6061 Al part during irradiation by a 0.6 msec pulse of 35 watts. This shows that current is emitted during the irradiation and collected during the plasma decay. The emitted current is a result of photoelectrons and thermoelectrons while plasma decay contributes to the collected current. This figure is included only for completeness since the current measurements require extensive shielding which was impossible during observations using the high speed video system.

Figure 8 is a composite of the high speed video data for 1100 Al, 7.8 msec pulse length and 325 watts of power. The sequence begins with the six segments in the top right position and proceeds right to left and top to bottom. Within each six segments the initial segment is at the right. Only 5.5 msec of data are presented since several frames have no plasma until initiation. The first frame is shown to indicate how timing is achieved. This figure illustrates very well the plasma initiation, propagation, decay and the reinitiation of additional plasmas. It is also evident that initiation can occur while more than one previous plasma is in existence. This photograph illustrates the existence of multiple plasmas during one laser welding pulse. All video recordings showed that this phenomenon occurred.

Using both the PMT signals and the high speed video the number of plasmas generated during one laser pulse were determined. In general there was no pattern for correlation between PMT and video data. (i.e. one did not consistently yield more detectable plasmas than the other nor did they consistently agree). The observed differences in the number of detectable plasmas is expected on the basis of plasma expansion and propagation as well as the effect of radiation intensity on the video recording. However comparing the data does permit better trends to be determined.

Figure 9 is a graph of the number of observed plasmas versus average laser power. These data show that the Al alloys as a group behave similarly to the 304 stainless steel but have higher thresholds. As expected from plasma initiation data (figure 6) the Al does not produce a plasma until higher power is used. Furthermore there are not as many plasmas generated on Al as there are on 304 stainless steel. For all materials studied higher power produced more plasmas.

The effect of input power (and thus the number of plasmas) upon melting is shown in figure 10. Here the melt depth as determined from metallography is shown as a function of laser power. The depth in 304 stainless steel appears to be linear with power while for Al it appears to have a threshold at about 300 watts followed by a rapid increase in depth.

Plots of the melt depth versus the number of plasmas generated for 304 stainless steel and 1100 Al show that 1 to 3 plasmas produce 0.25 to 0.33 mm of melt depth. Including 6061 Al in the analysis along with 1100 Al and 304 stainless steel requires including 9 plasmas to encompass meld depths of 0.25 to 0.36 mm. At this time there is not sufficient data to correlate melt depth with the number of plasmas generated.

Summary and Conclusions

A model is described which explains enhanced coupling in terms of the plasma generated during laser processing of materials. The model describes the plasma as a LSC wave preceeded by a pressure wave. The model also incorporates the creation of multiple plasmas during one laser pulse. Acoustical, optical, electrical and video observations of the laser generated plasma support the model.

The existence of the initial pressure wave and its subsequent regeneration with each new LSC wave help explain the large number of signals seen in acoustic emission monitoring of laser welds.[1] Each pressure wave will impinge upon the target as will reflections of these waves from surrounding reflectors and create an acoustic signal in the target. These signals must then be sorted from acoustic signals generated within the material itself. With this information it may now be possible to better correlate weld morphology with acoustic emission data.

Additional work must be done to fully characterize the plasma and methods developed to further enhance heat input to parts.

Acknowledgements

We thank Mr. L. Bryant, Jr. and Mr. J. P. Lucero of Los Alamos National Laboratory for the use training and support of the Spin Physics video system. We thank Mr. M. Ward of EG&G Los Alamos for his support in setting up the optical measuring systems. We also thank Mr. C. R. Tallman of the Los Alamos National Laboratory for the use of his acoustic microphones.

References

1. A. A. Boni, F. Y. Su, P. D. Thomas and H. M. Musal, Theoretical Study of Laser Target Interaction. Final Report April 1977, SAI-77-567LJ, Science Applications Inc.

2. A. N. Pirri, N. H. Kemp, R. G. Root and R. K. S. Wu, Theoretical Laser Effects Studies, Final Report, Jan. 1977, PSI-TR-89, Physical Sciences Inc.

3. G. K. Lewis, A. Rollett, L. Schwalbe, F. Flick and W. Ward (April, 1983) Acoustic Emission and Plasma Light Source Monitoring of Laser Welds, Presented at American Welding Society Meeting April 1983.

4. R. D. Dixon and G. K. Lewis, Plasma Monitoring of Laser Welds, to be published in The Welding Journal.

5. J. P. Jackson and P. E. Nielson, Ignition Transients and two-dimensional effects in the propagation of Laser Supported Absorption waves, Laser Digest, Spring 1974, AFWL-TR-74-100.

Figures

Autobiography

R. D. Dixon

Mr. R. D. Dixon has a BS in Mathematics and a MS in Physics from The University of South Dakota. He has been an instructor of physics at the University of Wisconsin, Superior; Optical Physicst, Chrysler Corp.; and Research Physicst and Manager, Rockwell International. He is presently a staff member in Process Metallurgy at the Los Alamos National Laboratory where he is involved with Laser and Electron Beam Welding research.

G. K. Lewis

Mr. G. K. Lewis has a Professional Engineering degree in Metallurgy from The Colorado School of Mines He has been a Senior Metallurgist with Pratt and Whitney Corporation. He is presently a staff member in Process Metallurgy at the Los Alamos National Laboratory where he is involved with Laser welding research.

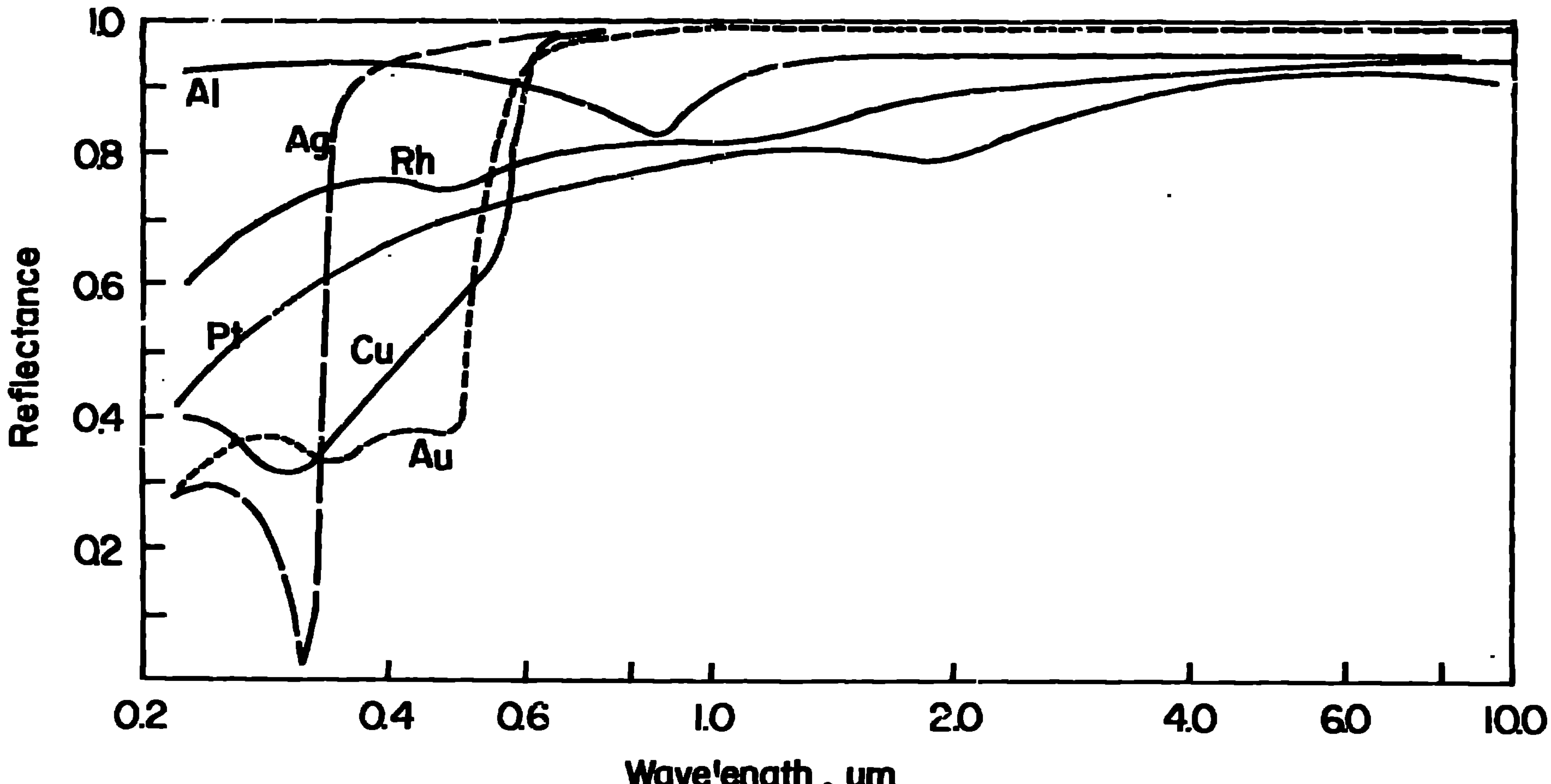

1.0
0.8
0.6
0.4
0.2
Reflectance
Al
Ag
Rh
Pt
Cu
Au
0.2
0.4
0.6
1.0
2.0
4.0
6.0
10.0
Wavelength , μm

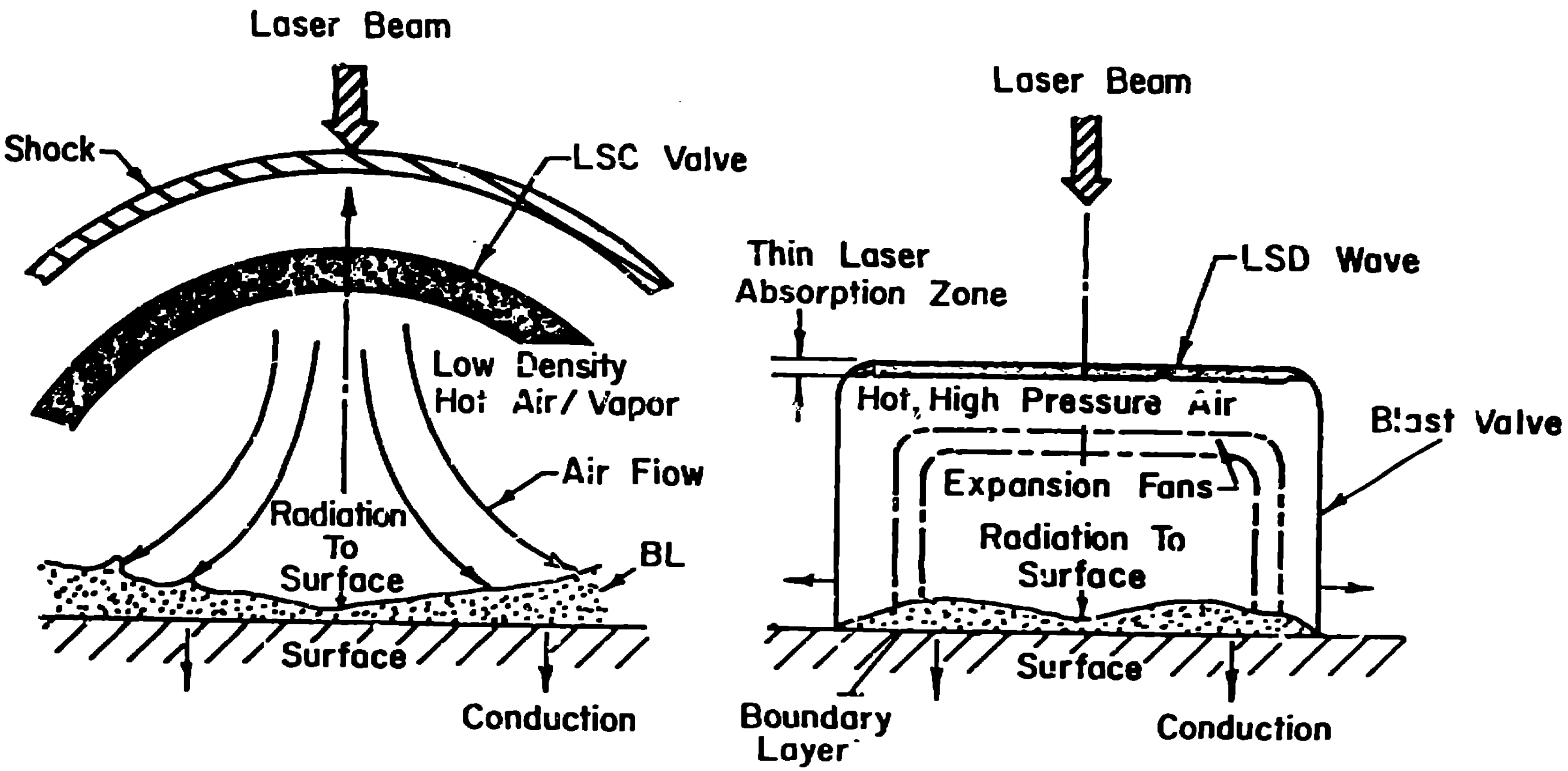
Laser Beam
Shock
LSC Valve
Low Density Hot Air/ Vapor
Air Flow
Radiation To Surface
BL
Surface
Conduction
Laser Beam
Thin Laser Absorption Zone
LSD Wave
Hot, High Pressure Air
Blast Valve
Expansion Fans
Radiation To Surface
Surface
Boundary Layer
Conduction

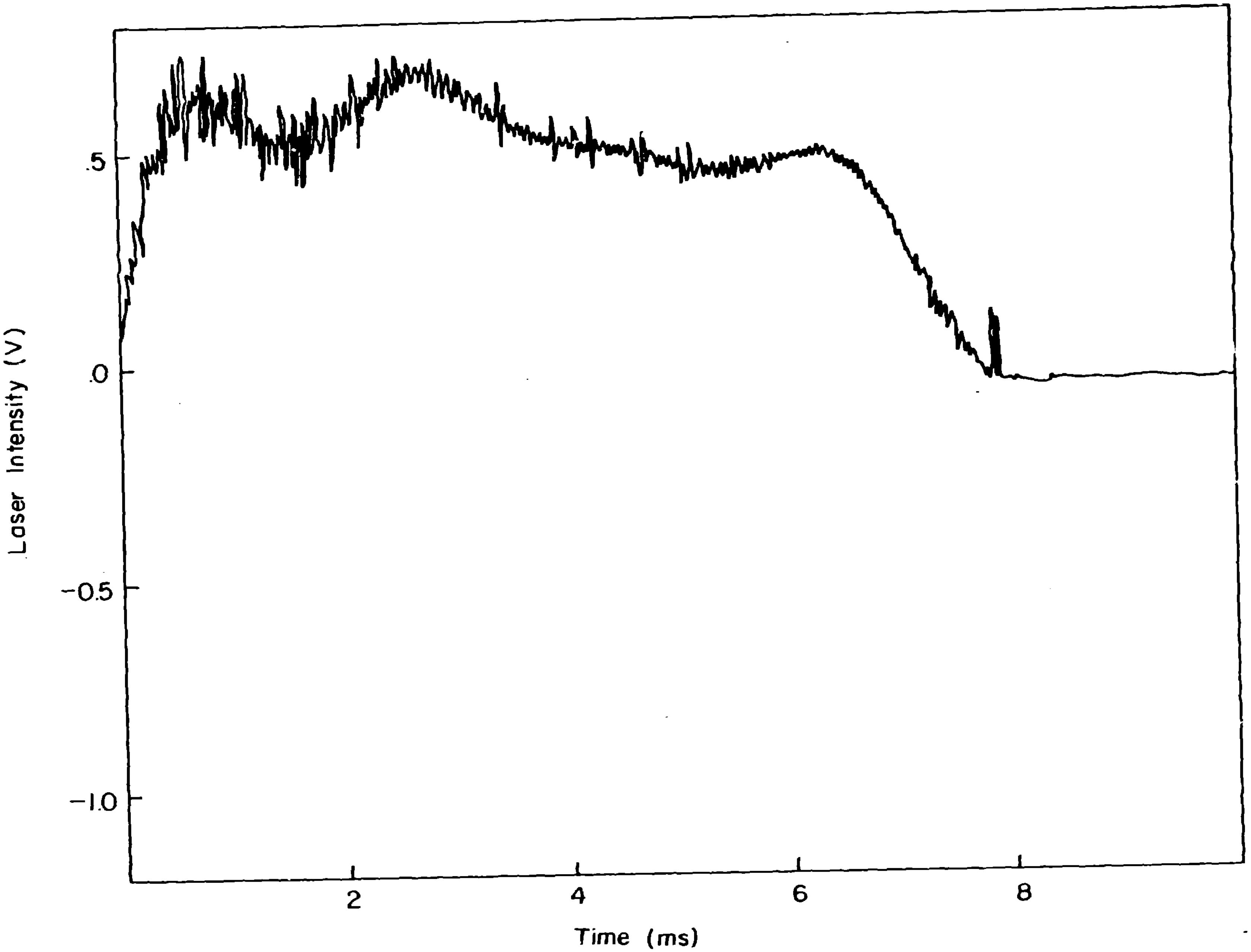

.5
.0
−0.5
−1.0
Laser Intensity (V)
2
4
6
8
Time (ms)

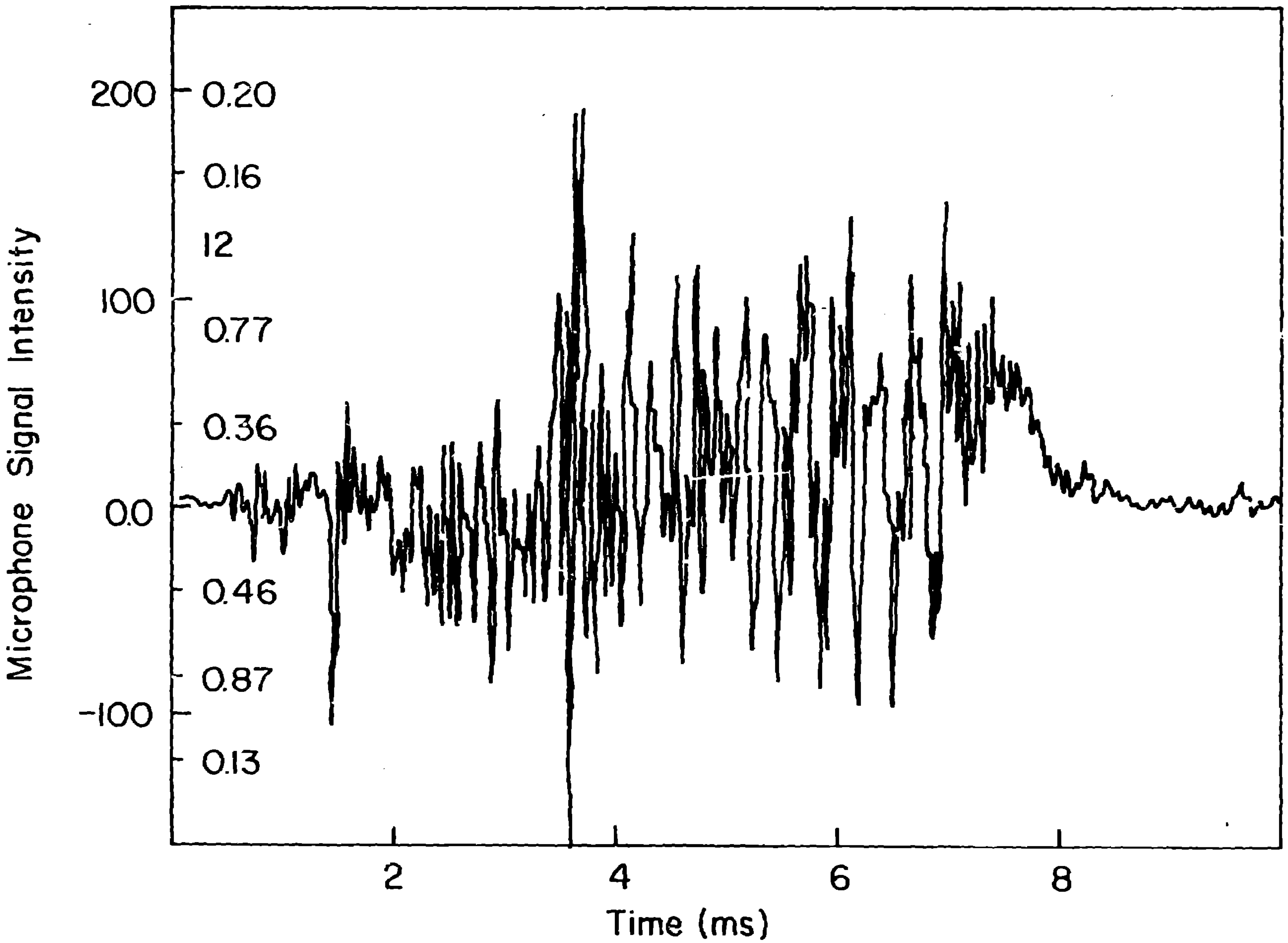
Microphone Signal Intensity
200
0.20
0.16
12
100
0.77
0.36
0.0
0.46
0.87
-100
0.13
2
4
6
8
Time (ms)

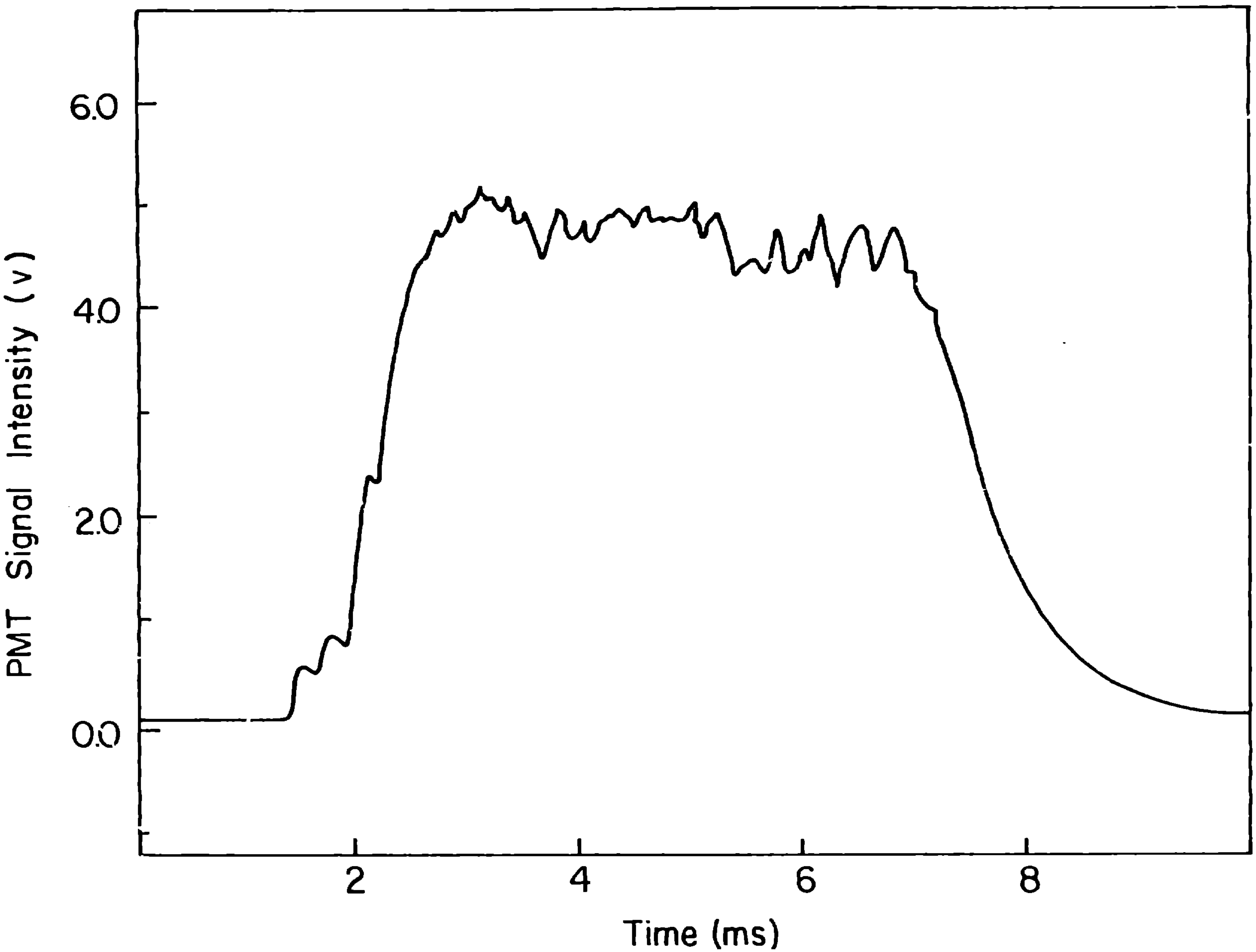
6.0
4.0
2.0
0.0
PMT Signal Intensity (v)
2
4
6
8
Time (ms)

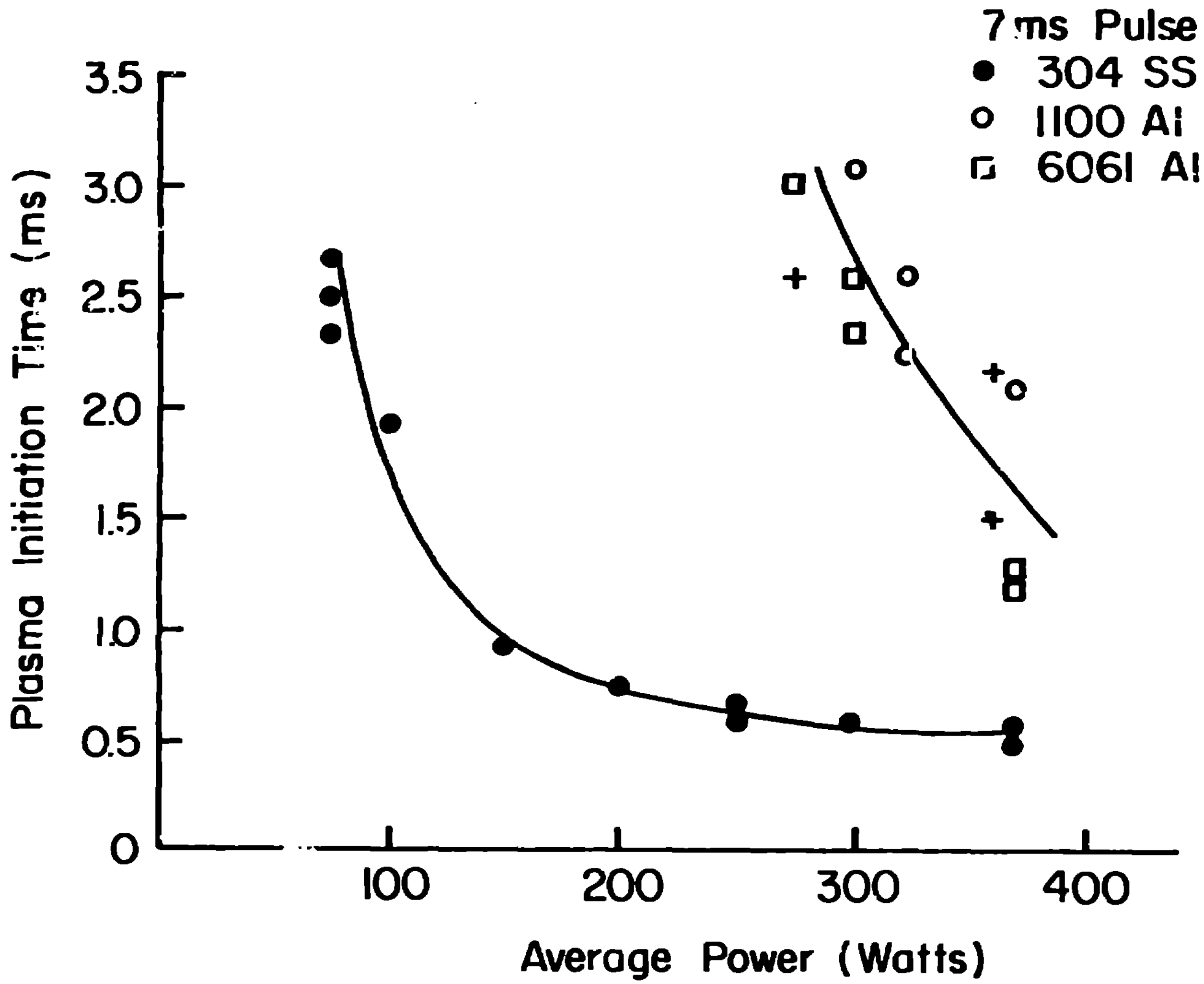

7 ms Pulse
304 SS
1100 Al
6061 Al
Plasma Initiation Time (ms)
3.5
3.0
2.5
2.0
1.5
1.0
0.5
0
100
200
300
400
Average Power (Watts)

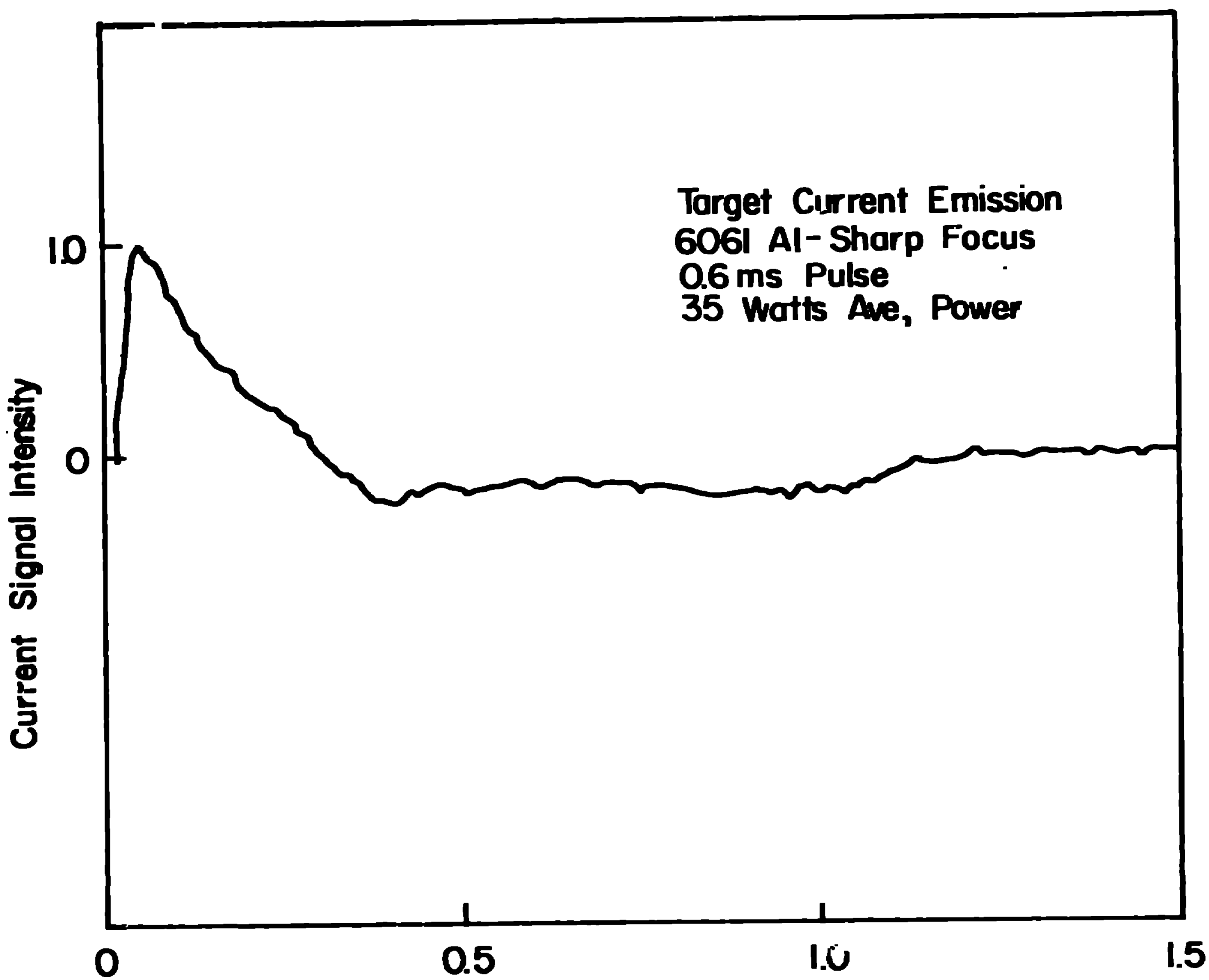

Target Current Emission
6061 Al-Sharp Focus
0.6 ms Pulse
35 Watts Ave, Power
Current Signal Intensity
1.0
0
0
0.5
1.0
1.5

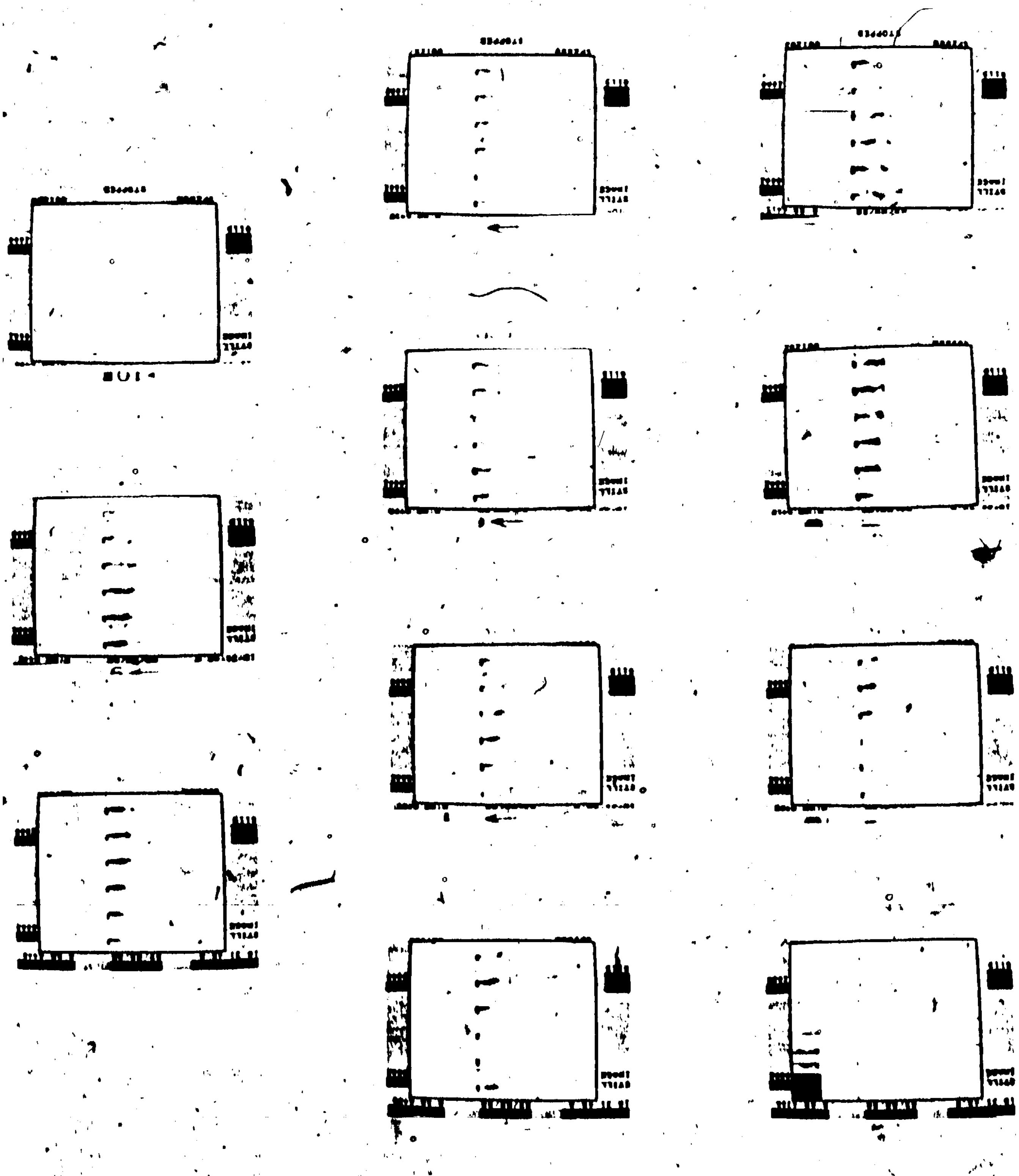

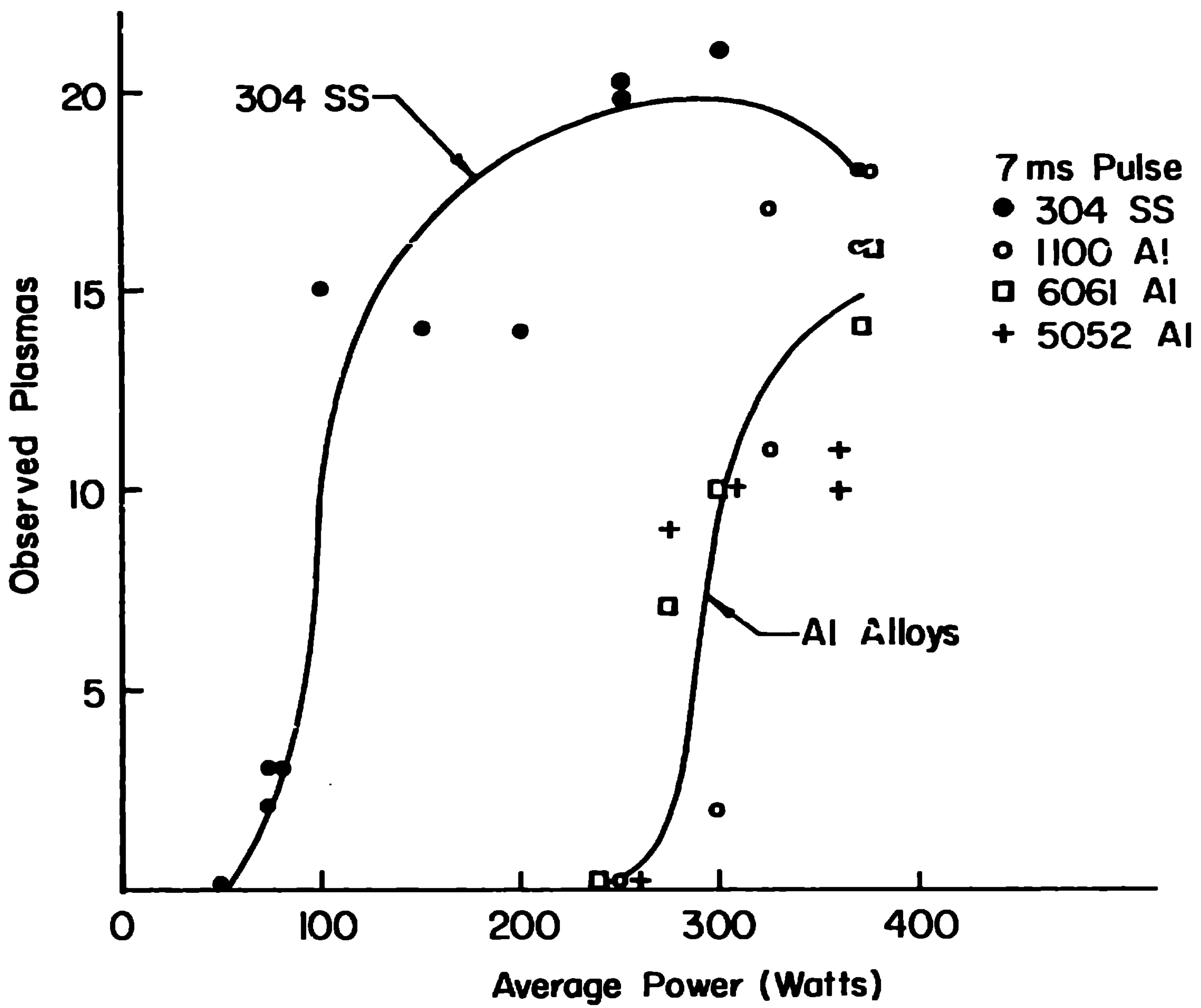

304 SS
Al Alloys
7 ms Pulse
304 SS
1100 Al
6061 Al
5052 Al
Observed Plasmas
Average Power (Watts)
0
100
200
300
400
5
10
15
20

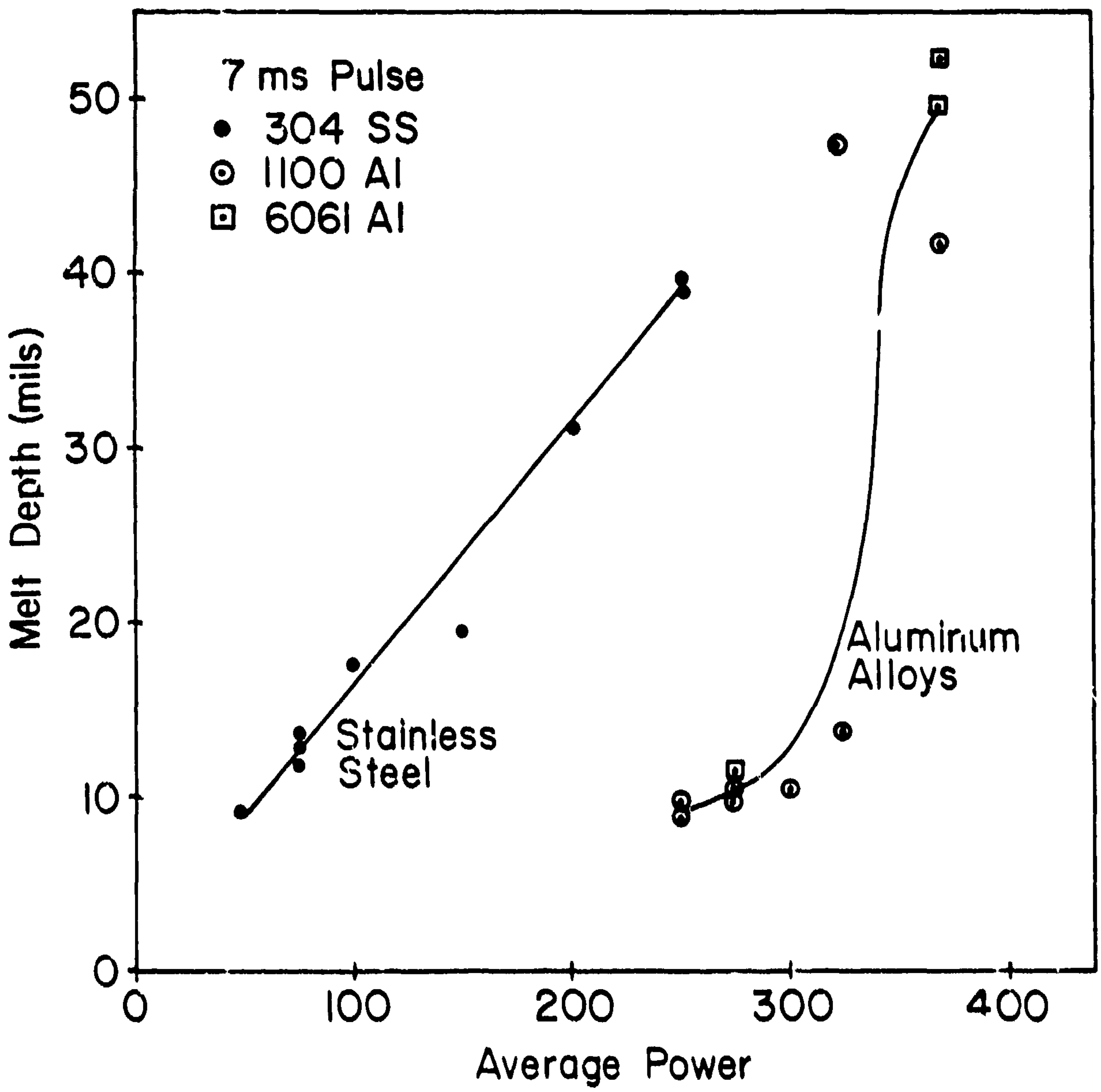
7 ms Pulse
304 SS
1100 Al
6061 Al
Melt Depth (mils)
Average Power
Stainless Steel
Aluminum Alloys
0
10
20
30
40
50
0
100
200
300
400